Efficient Production and Applications of 2- to 10-keV X Rays by Laser-Heated "Underdense Radiators"

L. J. Suter *M. S. Maxon*

R. L. Kauffman *J. F. Davis**

Introduction

Within the next decade, very-high-power, high-energy laser facilities may be constructed in Europe[1,2] and the United States.[3] Two-dimensional (2-D) numerical simulations with the LASNEX code[4] at Lawrence Livermore National Laboratory (LLNL) indicate that this next generation of lasers offers the prospect of producing multi-keV x rays with unprecedented efficiency: as much as 14% above 10 keV, 30% above 4 keV. Such efficiencies, coupled with the intrinsically high energy of these facilities, should allow us to produce great quantities of multi-keV x rays—as much as several hundred kilojoules. This, in turn, may allow us to perform experiments and field diagnostics we could never consider with current facilities. Applications of high-energy, multi-keV sources with the proposed National Ignition Facility (NIF) include volume preheating of experimental targets; bright, multi-keV backlighting; pumps for fluorescent imaging of capsule dopants and Doppler velocimetry; and uniform irradiation of large test objects for Nuclear Weapons Effects Testing (NWET).

Projections of Efficiency

Conventional slab targets irradiated by current lasers produce multi-keV x rays with relatively low efficiency. At photon energies >3 keV, the typical efficiency for converting laser light into multi-keV x rays is less than 1%.[5] Multi-keV efficiencies well in excess of those commonly obtained today are predicted to be achieved with "underdense radiators," a nontraditional source of laser-generated x rays (so called because the density of these targets is less than critical density of the laser light). Figure 1 shows two examples of such sources. Figure 1(a) is a column of gas (or foam) irradiated from one end by a single 0.35-μm (blue) laser beam. In simulations using 0.01 g/cm^3 of Xe gas irradiated by a 2-ns flattop pulse at an intensity of 10^{15} W/cm^2, we find

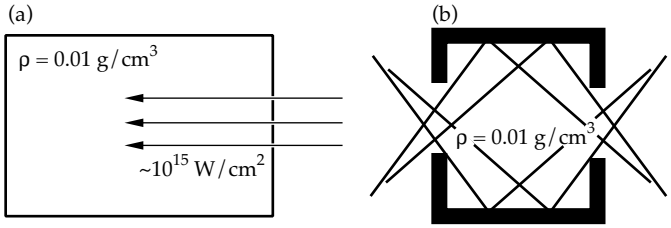

FIGURE 1. Two types of "underdense radiators." (a) is a gas (or foam) column irradiated from one end with a single, large-*f*-number beam. (b) is a transparent container, filled with underdense gas or foam, irradiated with several beams. NIF target type (a) can be irradiated with, at most, 10 TW. Target type (b) can accept several beams, so it can be irradiated with higher total power. (20-03-0696-1296pb01)

efficiencies into photons of energy >4 keV (L-shell Xe and continuum) to be 19% with a 10-TW beam. Since a cluster of four "beamlets" of the proposed National Ignition Facility (NIF)[3] will deliver 10 TW in the geometry of Fig. 1(a), good efficiency may be achievable with such gas-column sources. However, simulations indicate that higher efficiencies and higher photon energies with such a target will require more than 10 TW. This would be incompatible with the 10-TW/beam maximum of the NIF. Figure 1(b) shows a higher power source compatible with the NIF. It is a low-*Z* container, transparent to x rays of interest, filled with an appropriate-*Z*, low-density gas or foam. Since it is heated by more than one beam, it can be irradiated at much more than 10 TW. In simulations where the can is filled with Xe gas at 0.01 g/cm^3, we find near-optimal performance for containers 2 mm diameter and 1.6 mm long with 1-mm-diam laser entrance holes. For 2-ns pulses, simulated, >4-keV efficiencies range from 17% at 20 TW to 30% at 60 TW.

We have efficient 2-D designs of target type (b) at photon energies up to ~10 keV. Table 1 summarizes our LASNEX study. In all cases, the densities are 0.01 g/cm^3, and the rest of the laser energy appears as either thermal emission (<1 to 2 keV) or plasma energy.

*Alme Associates, Alexandria, VA.

Figure 2 plots the highest source efficiencies in the third column of Table 1 vs photon energy and compares them with current disc backlighter efficiencies.[5] The figure forcefully illustrates how much more efficient underdense radiators, heated by powerful lasers, can be compared to current backlighters.

TABLE 1. Summary of LASNEX study results.

Material	Power (TW)	Fraction of laser energy > $h\nu$ (keV)
Kr	60	4% > 13; 30% > 2
Ge	60	14% > 10; 26% > 2
Ge	50	10% > 10; 26% > 2
Ge	30	7% > 10; 20% > 2
Cu	40	11% > 8.5; 26% > 2
Cu	30	10% > 8.5; 24% > 2
Dy	60	9% > 8; 24% > 2
Xe	60	30% > 4; 48% > 1
Xe	50	26% > 4; 48% > 1
Xe	30	22% > 4; 40% > 1
Xe	20	17% > 4; 37% > 1

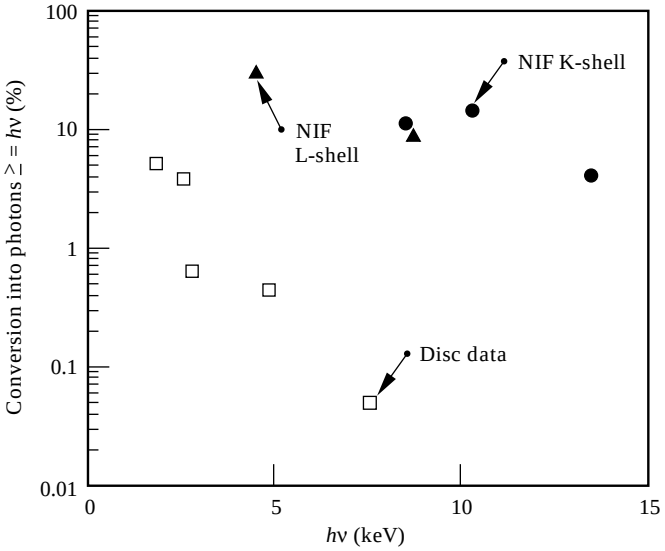

FIGURE 2. The projected multi-keV efficiencies for sources like those of Fig. 1(b) are much higher than current disc efficiencies. K-shell refers to the Ge, Cu, and Kr sources of Table 1. L-shell refers to the Dy and Xe sources. (20-03-0696-1301pb01)

Physics of Efficient Production

Analysis of LASNEX simulations leads to a simple understanding of such high efficiencies in the multi-kilovolt regime and tells us why these are qualitatively different from standard discs. In the following discussion, we use Xe as an example, although the arguments are valid for other materials as well.

Good Multi-KeV Efficiency Is Intrinsically Possible

First, we show how high, multi-keV efficiency is possible with an underdense radiator. Figure 3 illustrates the first component of high, multi-keV efficiency. It shows theoretical estimates of Xe emission at electron temperatures of 2 keV and at 5 keV. The Xe density is 0.01 g/cm^3. This plot makes a widely known but essential point: x-ray emission shifts to higher energy as plasma is made hotter. Figure 4, which plots radiation production/cm^3 vs electron temperature, contains the next step in the argument. This is from an optically thin LASNEX simulation. The black line is total emission vs T_e. The gray line is the emission >4 keV (see Fig. 3). This plot shows that the overall radiation production does not change greatly with plasma temperature. However, at higher temperatures almost all the emission will be multi-keV (see Fig. 3). Figure 4 illustrates an important point: a material that efficiently produces x rays in the softer, "thermal" region may also efficiently

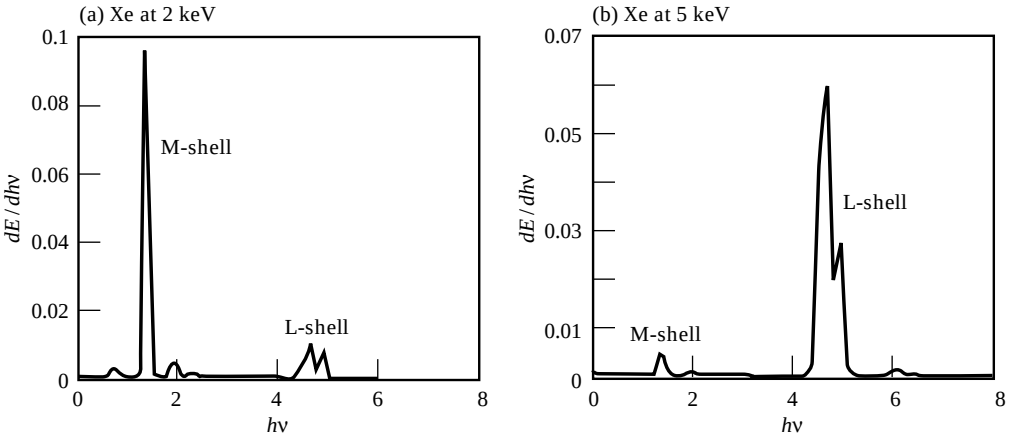

FIGURE 3. Emission from 0.01 g/cm^3 Xe at electron temperatures of (a) 2 keV and (b) 5 keV, simulated by XSN. Heating a material causes more of its total emission to be produced at higher photon energies. (20-03-0696-1302pb01)

produce x rays in a much more energetic region if it is made hotter.

Figure 5 is the plot needed to reach a simple, quantitative understanding of efficient multi-keV production. It shows Xe L-shell radiation production vs electron density for material at electron temperatures of 3, 4 and 5 keV. The Xe volume is that of a 1.4-mm-radius standard "gasbag"[6] similar to ones we have shot on Nova for studies of laser–plasma instabilities.[7] Figure 5 shows that at densities ~1 to 1.5×10^{21}/cm, a 4- to 5-keV Xe-filled gasbag would produce ~5 to 12 TW of L-shell emission. Thus, if we can heat such a gasbag to these temperatures with a 30-TW, 1-ns Nova pulse (30 kJ energy), and if it remains together for ~1 ns, we might expect to produce ~5 to 10 kJ of L-shell emission, or 16 to 33% multi-keV efficiency.

That we can both heat the bag and that it does not disassemble too quickly follow from simple arguments. If all the material in the gasbag is at constant temperature, then its thermal energy in kJ is approximately $2.75T_e$ (in keV) $\times n_e$ (in units of 10^{21}/cm^3). For the temperature and density regimes of interest (4 to 5 keV, 1 to 1.5×10^{21}), this corresponds to 10 to 20 kJ. Moreover, the sound speed of Xe gas at 4 keV is ~6×10^7 cm/s, so the rarefaction takes more than 1 ns to propagate to the center of the 1.4-mm-radius bag.

The Xe emission calculations just discussed were made with a non–local-thermodynamic-equilibrium average-atom model known as XSN.[8] Better theoretical estimates using a detailed configuration approximation model[9] give essentially the same result. Our estimates above also assume the radiation can get out. Detailed simulations with radiation transport of the lines indicate that the radiation can escape.

Hydrodynamics for Good Efficiency

Above we reasoned that efficient multi-keV radiation production is possible. It also indicates that the achievement of good multi-keV efficiency requires a hydrodynamic system that converts most of the laser energy into hot plasma at sufficient density that it can radiate a considerable fraction of the energy before it disassembles. Underdense plasmas can provide such a hydrodynamic system. Moreover, they do this better than discs, which is the main reason underdense plasmas can be considerably more efficient multi-keV sources than discs (see Fig. 2).

We can see the hydrodynamic differences by analyzing three simulated Xe gas-column sources of different densities (0.01, 0.02 and 0.1 g/cm^3) but irradiated by the same laser. Figure 6 shows the total L-shell radiation escaping 1-D simulations of these gas columns vs time. (1-D analogs of the 2-D gas column of Fig. 1[a]. The 1-D efficiency is higher than 2-D efficiency because there is no radial hydrodynamic disassembly.) The gas column that started at 0.01 g/cm^3 (~$0.2n_c$ when fully ionized) has the highest efficiency. At the

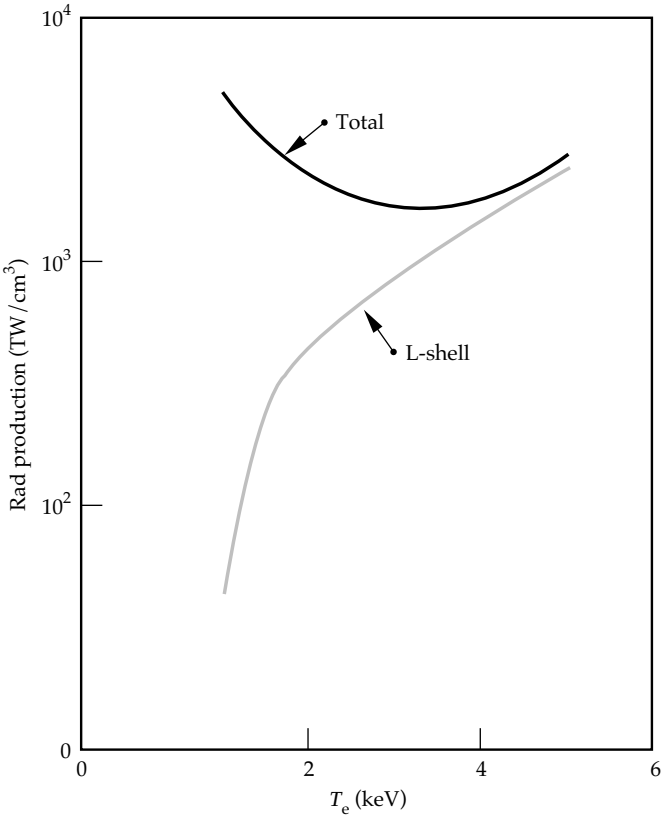

FIGURE 4. Total emission per cm^3 vs electron temperature and L-shell emission (Xe at 0.01g/cm^3). A material that is an efficient source of thermal x rays can also be a good source of multi-keV x rays, if we can make it hot enough. (20-03-0696-1303pb01)

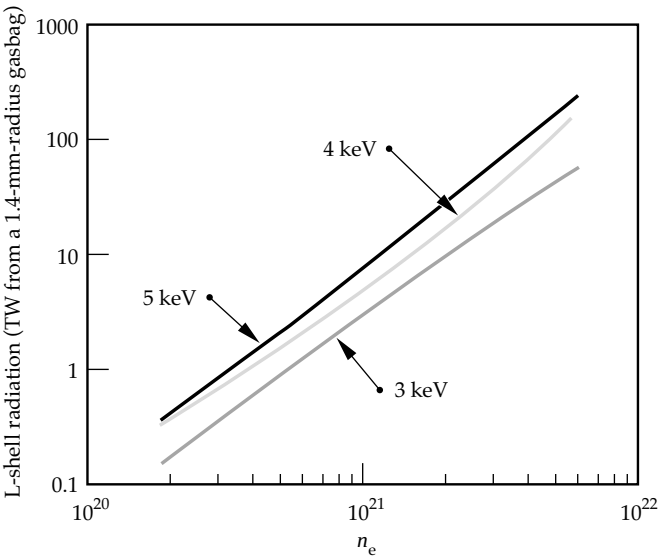

FIGURE 5. L-shell emission from the volume of a 1.4-mm-radius, Xe-filled gasbag, vs electron density. (20-03-0696-1304pb01)

end of the 2-ns pulse, more than half of the incident 48-TW laser power is escaping this column as L-shell emission. The column that started at 0.02 g/cm^3 behaves like the lower density one for ~1 ns, but then its efficiency drops notably. The 0.1-g/cm^3 gas column has comparatively low efficiency the whole time. We call it disc-like since its simulated L-shell radiation production is the same as a frozen Xe slab's (not shown).

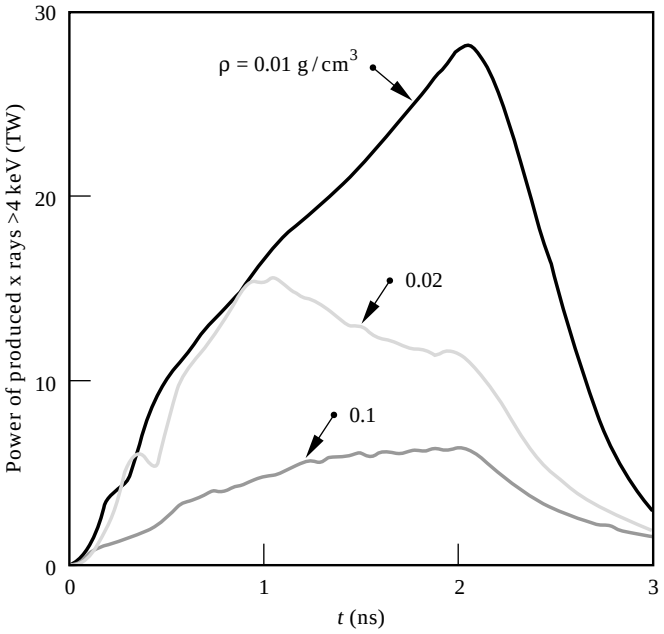

FIGURE 6. Time dependence of L-shell emission escaping 1-D LASNEX simulations of Xe gas columns of different densities. The three columns were all irradiated with 48 TW of blue laser light. (20-03-0696-1305pb01)

Now we can pass on to the next level of understanding. Figure 7 plots electron density and temperature, at 1 ns, vs length along the gas columns. The three 1-D gas columns clearly have very different hydrodynamics. In Fig. 7(a), in the 0.01-g/cm^3 gas column, the heating front moves nearly supersonically (also known as a bleaching front). However, in the poorest-efficiency, 0.1-g/cm^3 gas column, Fig. 7(b), the heating front moves subsonically (also known as an ablative front). Unlike the bleaching front, the ablative front drives a shock of dense material ahead of itself. The 0.02-g/cm^3 gas column is a transitional case; early in time it was heating in an approximately supersonic manner. However, residual hydrodynamics caused a density bump ahead of the front to accumulate, finally causing a transition, at ~1 ns, to completely ablative heating. The transition from bleaching to ablative coincides with the efficiency drops at 1 ns seen in Fig. 6.

Further analysis shows that a bleaching front creates far hotter plasma than an ablative front, hotter plasma that is denser and therefore more efficient in producing multi-keV x rays. In particular, we find the following:

- In producing a given mass of hot plasma, more energy is lost to low-photon-energy radiation when the heating occurs in a dense ablation front than when the matter is heated in the uncompressed bleaching front. The ablative front's dense material, which is being heated by conduction from the laser-deposition region, has a very high radiation production rate. However, since it is relatively cold, the emission is not multi-keV. This emission is energy lost from the system that cannot contribute to heating plasma and, since it is low-photon energy, does not contribute to multi-keV production. From the viewpoint of multi-keV radiation production, it is a parasitic loss.

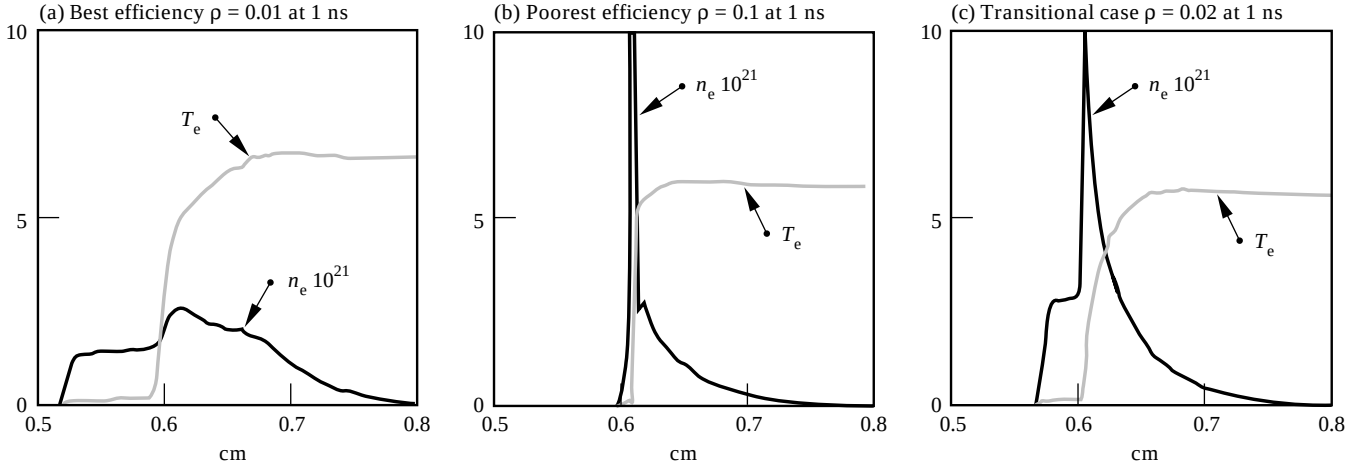

FIGURE 7. Electron temperature (keV) and electron density ($\times 10^{21}$) at 1 ns vs axial position (cm) for the three 1-D gas-column sources in Fig. 6. (20-03-0696-1306pb01)

- Because of the higher density, the material in the ablation front rises to higher pressure. This ends up as more kinetic energy per unit of mass heated.
- More kinetic energy causes the hot blowoff behind an ablative heating front to be less dense than behind a bleaching front; compare electron density profiles of Fig. 7(a) and 7(b). Consequently, the blowoff behind the bleaching front produces more coronal, multi-keV x rays per unit mass because such emission scales approximately as $(n_e)^2$ (see Fig. 5).

Experimental Validation of Modeling

Calculations similar to those above provided the first indication that we might be able to very efficiently produce multi-keV x rays with laser-heated underdense sources.[10] Following these initial findings, we performed theoretical and experimental work to examine the validity of these predictions. This involved testing our ability to properly estimate the multi-keV efficiencies of published slab data,[11–13] as well as efficiencies from Xe-filled gasbags[6] specifically shot at Nova to test these predictions.[14] Figure 8 compares simulated and experimental absolute multi-keV efficiencies for all these experiments. Except for two low-intensity (1.4×10^{14} W/cm^2) slab targets, there is general agreement between the experiment and simulations. In particular, the >4 keV, L-shell production from our Xe gasbag experiments[14] agrees satisfactorily with the 2-D LASNEX estimates. They are actually slightly higher than the simulations. This favorable comparison seems to lend credibility to the predictions discussed above.

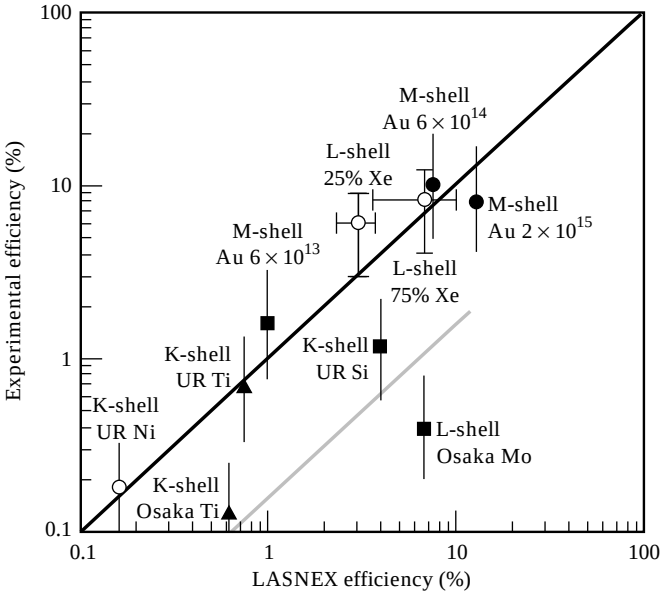

FIGURE 8. Comparison of simulated and experimental multi-keV conversion efficiencies from several databases. (20-03-0696-1307pb01)

In addition to this comparison with experiment, there is a fairly extensive and documented database indicating that LASNEX reasonably models the electron temperature in gasbags and gas-filled hohlraums.[15] The capacity to properly estimate underdense plasma electron temperatures is an essential component of believable, multi-keV predictions.

Applications of Efficient Multi-KeV X-Ray Sources

Below we discuss four applications of high-energy, multi-keV sources with the NIF:

1. Volume preheating of experimental targets.
2. Bright, multi-keV backlighting.
3. Pumping for fluorescent imaging of capsule dopants and doppler velocimetry.
4. Uniform irradiation of large test objects for NWET.

Preheat Sources

Multi-keV x rays can be used to preheat experimental packages. The preheat temperature T_e produced in a package located distance d away from a multi-keV source can be found by balancing x-ray deposition with internal energy. Neglecting ionization energy, this balance is approximately

$$\frac{\eta_x E_L}{4\pi d^2 \ell} = \left(\frac{3}{2}\right)\frac{\rho(Z+1)T_e}{A}\left(9\times 10^4\right) \quad . \tag{1}$$

Here η_x is the multi-keV efficiency; E_L is the laser power; ℓ is the scale length over which x-ray absorption occurs in the experimental package; ρ, Z, and A are the density, atomic number, and weight of the experiment we are preheating. Using $\eta_x = 30\%$, $E_L = 10^6$ J, $d = 0.5$ cm, $\rho = 1$ g/cm^3, and $(Z+1)/A = 0.33$ gives $T_e = 2$ eV-cm/ℓ. Depending on ℓ, it may be possible to preheat large $\rho = 1$ samples to ~5 eV and thinner ones up to several tens of eV, possibly approaching 100 eV. NIF applications for preheat sources like this include off-Hugoniot equation-of-state measurements and low-temperature hydrodynamics.

Backlighter Sources

Sources like these could serve as the bright, high-photon-energy, large-area backlighters needed for bigger targets. Consider, for example, the 60-TW Ge source listed in Table 1 scaled up to 100 TW (14% > 10 keV). Viewed from the end of the 2-mm-diam cylinder, the >10-keV emission/cm^2/sr will be 3.5×10^{13} W/cm^2/sr. This is equivalent to viewing a 10-keV hemi-isotropic

disc source of 1% efficiency irradiated by 700 TW at an intensity of ~2.2×10^{16} W/cm^2.

Pumps for Fluorescence-Based Diagnosis

Efficient multi-keV sources and high-power lasers may allow us to field fluorescence-based diagnostics—a qualitatively new way of studying hydrodynamics. The principle is simple: a multi-keV source at distance d pumps a dopant in a capsule. In imaging, the number of photons collected from a resolution element r is given by

$$\#\ \text{of photons} = \frac{\eta_x P_L}{4\pi d^2} r^2 \left(\frac{r}{\ell}\right) \frac{\frac{\eta_F}{4\pi}\delta\Omega\eta_{det}\delta\tau}{E_x} \quad . \qquad (2)$$

Here, P_L is the laser power; E_x, the source's average photon energy; η_F, the dopant's fluorescent efficiency; and $\delta\Omega$, η_{det}, and $\delta\tau$, the camera's solid angle, efficiency, and time resolution. Using r = 10 μm, P_L = 60 TW, η_x = 10%, E_x = 10 keV, d = 0.5 cm, $\delta\tau$ = 100 ps, and η_F = 0.2 (i.e., Cu-K at 8 keV has η_F = 0.2 in Ref. 16) gives

$$\#\ \text{of photons} = \left(3.2 \times 10^9\right)\left(\frac{10\,\mu\text{m}}{\ell}\right)\delta\Omega\eta_{det} \quad . \qquad (3)$$

For a 10-μm pinhole at 1 cm and the dopant concentration arranged so that $10\,\mu\text{m}/\ell \approx 0.01$ to 0.1, we collect 40 to 400 photons from each 10-μm resolution element. For a curved crystal/Rowland circle system, the number of photons could be ~300 to 3000, at 1% crystal reflectivity.

A compelling possibility is using doppler spectroscopy of fluorescent lines to measure pusher velocity and, possibly, show the evolution of turbulence (via line broadening) at stagnation. Figure 9 indicates how the fluorescent lines may be shifted when the pusher starts to move, during final acceleration, and during stagnation. A requirement for this will be an efficient spectrometer which sees only diametrically opposed parts of a doped capsule. Related to this, fluorescence might produce cutaway pictures of capsule mix, perhaps similar to those used to visualize mixing in 3-D simulations. At a velocity of 10^7 cm/s or more, narrowband Doppler imaging with a camera of spectral resolving power 1500 or greater[17,18] could image only one side of the imploding pusher.

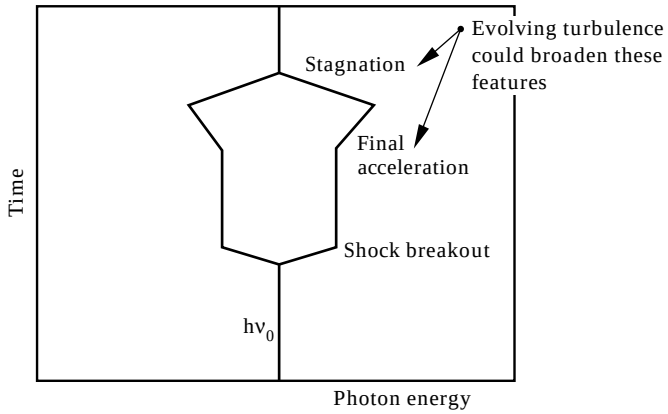

FIGURE 9. Doppler spectroscopy of fluorescing dopants in a capsule could measure pusher velocity and, possibly, show the evolution of turbulence, via line broadening, at stagnation. Efficient multi-keV sources could pump such fluorescence. (20-03-0696-1308pb01)

Large Fluence-Area Products with Good Uniformity

A requirement for NWET is that the flux over a test object be uniform to ±10%. This allows us to describe an NWET simulator by the fluence × area product that it can produce with that uniformity. In general, the fluence × area product in a given spectral region will be

$$\text{fluence} \times \text{area} = \left(\frac{E_L\eta}{4\pi}\right) T_{\text{debris-shield}}\left(\delta\Omega_{10\%}\right) \quad . \qquad (4)$$

The first term ($E_L\eta/4\pi$) is the source output per steradian in the spectral range of interest. It is determined by multi-keV source efficiency and total laser energy. $T_{\text{debris-shield}}$ is the debris shield transmission. It will be ~unity at 5 keV and higher, but may be significantly <1 at lower energies. The last term $\delta\Omega_{10\%}$ is the solid angle we can collect from each source and still get ±10% uniformity. It is a strong function of geometry. If all the emission is concentrated at a single point, as in typical pulse-power NWET simulators, we can collect only 0.45 sr with ±10% uniformity. However, if we produce x rays in a number of properly distributed sources, the useful solid angle increases. With four distributed sources, we can collect up to 1.6 sr from each source, and with 25 distributed sources, 4.5 sr. Thus, with proper facility capabilities, it is possible for 1 J of laser-produced multi-keV energy to be worth up to 10 J produced by a more conventional NWET simulation source. However, this improvement comes at a facilitization price. The sources need to be distributed over an area comparable to the size of the test object. For objects ~1 m across, this requires steering beams to irradiate sources much as 50 cm from chamber center.

On the NIF, the estimated fluence × area products with four distributed sources and 100% debris-shield transmission are as follows: 1 to 5 keV, 50,000 J-cm^2; 5 to 15 keV, 14,000 J-cm^2. With 25 distributed sources: 1 to 5 keV, 140,000 J-cm^2; 5 to 15 keV, 40,000 J-cm^2. This prospect for simulation capacity has led to the formation of a joint U.S. Department of Defense–Department of Energy working group (NIF Radiation Sources Users Group[19]) that works with the NIF Project aiming to optimize the NIF's NWET capabilities.

Acknowledgments

This work was supported by the Defense Nuclear Agency (Department of Defense) and the U.S. Department of Energy. We would like to acknowledge very useful discussions with Mike Tobin and Greg Simonsen of LLNL, C. P. Knowles of JAYCOR, and William Summa and Ralph Schneider of DNA.

Notes and References

1. M. Andrè, M. Novaro, and D. Schirmann, "Technologie pour un Laser Megajoule," *Review Scientifique et technique de la Direction des applications militaires*, Chocs, Numèro 13, 73, April 1995.
2. J. MacMordie, private communication (AWE, Aldermaston, UK, 1995).
3. J. T. Hunt et al., *A Design Basis for the National Ignition Facility*, Lawrence Livermore National Laboratory, Livermore, CA, UCRL-JC-117399 (1994).
4. G. B. Zimmerman and W. L. Kruer, *Comments Plasma Phys. Controlled Fusion* **2**, 51 (1975).
5. R. L. Kauffman, *Handbook of Plasma Physics, Vol. 3: Physics of Laser Plasma*, p. 123, Eds. M. N. Rosenbluth and R. Z. Sagdeev, Elsevier Science Publishers B. V. (1991).
6. R. L. Kirkwood et al., "Effect of Ion Wave Damping on Stimulated Raman Scattering in High Z Laser Produced Plasmas," *Phys. Rev. Lett*., accepted for publication.
7. B. J. MacGowan et al., *Phys Plasmas* **3**, 2029 (1996).
8. D. E. Post, R. V. Jensen, C. B. Tarter, W. H. Grasberger, and W. A. Lokke, *At. Data and Nuclear Data Tables* **20**, 397 (1977); G. B. Zimmerman and R. M. More, *J. Quant. Spectros. Radiat. Transfer* **23**, 517 (1980).
9. P. L. Hagelstein, *Physics of Short Wavelength Laser Design*, Lawrence Livermore National Laboratory, Livermore, CA, UCRL-53100 (1981).
10. L. J. Suter et al., "NIF will be a very useful DNA simulation facility just using laser produced x rays," *Proceedings of the NWET Applications for NIF Workshop*, G. Simonsen, Ed., Lawrence Livermore National Laboratory, Livermore, CA, March 15–17, 1994.
11. Kondo et al., *J. Appl. Phys*. **67**, 2693, (1990).
12. Yaakobi et al., *Opt. Commun*. **38**, 196 (1981).
13. R. L. Kauffman et al., *Laser Program Annual Report, 1986*, Lawrence Livermore National Laboratory, Livermore, CA, UCRL-50021-86 (1986).
14. R. L. Kauffman et al., *ICF Quarterly Report* **6**(2), Lawrence Livermore National Laboratory, Livermore, CA, UCRL-50021-96 (to be published fourth quarter, 1996).
15. L. V. Powers et al., *Phys. Plasmas* **2**, 2473 (1995).
16. S. T. Perkins et al., *Tables and Graphs of Atomic Subshell and Relaxation Data Derived from the LLNL Evaluated Atomic Data Library (EADL), z=1-100*, UCRL-50400 Vol. 30, Lawrence Livermore National Laboratory, Livermore, CA, October 31, 1991.
17. F. J. Marshall and J. Ortel, "A Framed Monochromatic X-Ray Microscope for ICF," *11th Topical Conference High Temperature Plasma Diagnostics*, Monterey, CA, May 12–16, CONF-960543-Absts., E-1, submitted to RSI.
18. S. A. Pikuz et al., "High-Luminosity Monochromatic X-Ray Backlighting Using Incoherent Plasma Source to Study Extremely Dense Plasma," *11th Topical Conference High Temperature Plasma Diagnostics*, Monterey, CA, May 12–16, CONF-960543-Absts., E-2, submitted to RSI.
19. Wendland Beezhold (SNLA), George Ulrich (DNA), and Greg Simonsen (LLNL), private communication (December, 1994).